

Modeling of the SET and RESET Process in Bipolar Resistive Oxide-Based Memory Using Monte Carlo Simulations

Alexander Makarov, Viktor Sverdlov, and Siegfried Selberherr

Institute for Microelectronics, TU Wien, Guhausstrae 27-29,

A-1040 Vienna, Austria

{makarov,sverdlov,selberherr}@iue.tuwien.ac.at

Abstract. A stochastic model of the resistive switching mechanism in bipolar oxide-based resistive random access memory (RRAM) is presented. The distribution of electron occupation probabilities obtained is in agreement with previous work. In particular, a low occupation region is formed near the cathode. Our simulations of the temperature dependence of the electron occupation probability near the anode and the cathode demonstrate a high robustness of the low occupation region. The RESET process in RRAM simulated with our stochastic model is in good agreement with experimental results.

Keywords: stochastic model, resistive switching, RRAM, Monte Carlo method.

1 Introduction

With memories based on charge storage (such as DRAM, flash memory, and other) approaching the physical limits of scalability, research on new memory structures has significantly accelerated. Several concepts as potential substitutes of the charge memory were invented and developed. Some of the technologies are already available as prototype (such as carbon nanotube RAM (NRAM), copper bridge RAM (CBRAM)), others as product (phase change RAM (PCRAM), magnetoresistive RAM (MRAM), ferroelectric RAM (FRAM), while the technologies of spin-torque transfer RAM (STTRAM), racetrack memory, and resistive RAM (RRAM) are under research. A new type of memory must exhibit low operating voltages, low power consumption, high operation speed, long retention time, high endurance, simple structure, and small size [1].

One of the most promising candidates for future universal memory is the resistive random access memory (RRAM). It is based on new materials, such as metal oxides [2-4] and perovskite oxides [5]. This type of memory is characterized by high density, excellent scalability, low operating voltages (< 2 V), fast switching times (< 10 ns), and long retention time. On the other hand, RRAM devices have not demonstrated yet sufficient endurance. Unless this problem can be solved, this technology is unlikely to be brought to market in the 2020 time-frame [1]. Unfortunately, a proper fundamental understanding of the switching

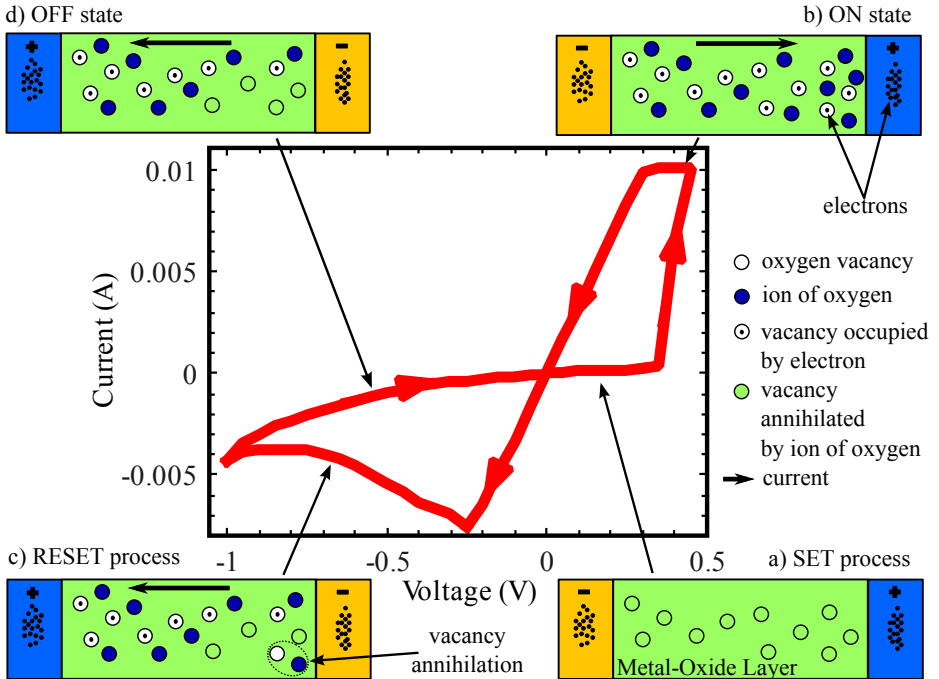


Fig. 1. Typical hysteresis cycle in RRAM and illustration of the resistive switching mechanism in bipolar oxide-based memory cell: (a) Schematic illustration of the SET process. (b) Schematic view of the conducting filament in the low resistance state (ON state). (c) Schematic illustration of the RESET process. (d) Schematic view of the conducting filament in the high resistance state (OFF state). Only the oxygen vacancies and ions that impact the resistive switching are shown.

mechanism in resistive random access memory (RRAM) is still missing, despite the fact that several physical mechanisms based on either electron or ion determined switching have been recently suggested in the literature: a model based on trapping of charge carriers [6], electrochemical migration of oxygen vacancies [7, 8], electrochemical migration of oxygen ions [9, 10], a unified physical model [11, 12], a domain model [13], a filament anodization model [14], a thermal dissolution model [15], and others.

In this work we present a stochastic model of the bipolar resistive switching mechanism based on electron hopping between the oxygen vacancies along the conductive filament in an oxide layer.

2 Model Description

We associate the resistive switching behavior in oxide-based memory with the formation and rupture of a conductive filament (CF) (Fig. 1).

The CF is formed by localized oxygen vacancies (V_o) [11, 12] or domains of V_o . Formation and rupture of a CF is due to a redox reaction in the oxide layer under a voltage bias. The conduction is due to electron hopping between these V_o .

For modeling the resistive switching in bipolar oxide-based memory by a Monte Carlo method, we describe the dynamics of oxygen ions (O^{2-}) and electrons in an oxide layer as follows:

- formation of V_o by O^{2-} moving to an interstitial position;
- annihilation of V_o by moving O^{2-} to V_o ;
- movement of O^{2-} between the interstitials;
- an electron hop into V_o from an electrode;
- an electron hop from V_o to an electrode;
- an electron hop between two V_o .

In order to model the dependences of transport on the applied voltage and temperature we choose the hopping rates for electrons as [16]:

$$\Gamma_{nm} = A_e \cdot \frac{dE}{1 - \exp(-dE/T)} \cdot \exp(-R_{nm}/a), \quad (1)$$

Here, A_e is a coefficient, $dE = E_n - E_m$ is the difference between the energies of an electron positioned at sites n and m , R_{nm} is the hopping distance, a is the localization radius. The hopping rates between an electrode (0 or $N + 1$) and an oxygen vacancy m are described as [12]:

$$\Gamma_m^{iC} = \alpha \cdot \Gamma_{0m}, \Gamma_m^{oC} = \alpha \cdot \Gamma_{m0}, \quad (2)$$

$$\Gamma_m^{iA} = \beta \cdot \Gamma_{(N+1)m}, \Gamma_m^{oA} = \beta \cdot \Gamma_{m(N+1)}, \quad (3)$$

Here, α and β are the coefficients of the boundary conditions on the cathode and anode, respectively, N is the number of sites, A and C stand for cathode and anode, and i and o for hopping on the site and out from the site, respectively.

To describe the motion of ions we have chosen the ion rates similar to (1):

$$\Gamma'_n = A_i \cdot \frac{dE}{1 - \exp(-dE/T)}, \quad (4)$$

Here we assume hopping only on a nearest interstitial. Thus, a distance-dependent term is included in A_i . dE includes the formation energy for the m -th V_o /annihilation energy of the m -th V_o , when O^{2-} is moving to an interstitial or back to V_o , respectively.

The current generated by hopping is calculated as:

$$I = q_e \cdot \sum dx / \sum \left(1 / \sum_m \Gamma_m \right) \quad (5)$$

Here q_e is the electron charge.

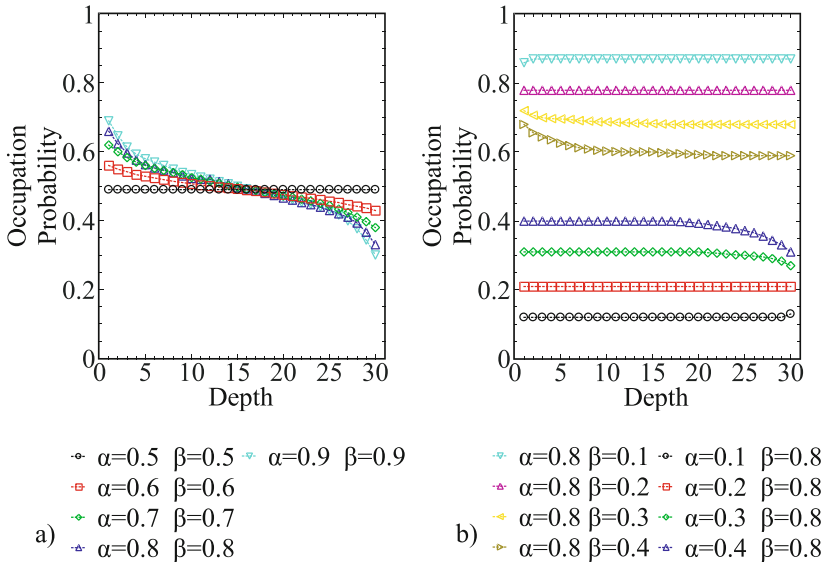


Fig. 2. Calculated distributions of electron occupation probabilities for unidirectional next nearest neighbor hopping between the V_o (the 1st V_o is near the cathode, the last V_o is near the anode): (a) $\alpha > 0.5$ and $\beta > 0.5$, $p_c = 0.5$; (b) $\beta < 0.5$ and $\beta < \alpha$, $p_c = 1 - \beta$; $\alpha < 0.5$ and $\alpha < \beta$, $p_c = \alpha$

3 Model Verification

Calculations are performed on one-dimensional lattices. All V_o are at the same energy level, if no voltage is applied. For simplify the calculations we assume that the oxygen vacancy is either empty or occupied by one electron.

3.1 Calculation of Electron Occupation Probabilities

To verify the proposed model, we first evaluate the average electron occupations of hopping sites under different conditions. For comparison with previous works all calculations in this subsection are made on a lattice consisting of thirty equivalent, equidistantly positioned hopping sites V_o .

Following [17], we first allow hopping in one direction and only to/from the closest V_o . The occupation probability of the central oxygen vacancies, p_c , is described depending on the boundary conditions as follows: 1) for $\alpha > 0.5$ and $\beta > 0.5$, $p_c = 0.5$; 2) for $\alpha < 0.5$ and $\alpha < \beta$, $p_c = \alpha$; 3) for $\beta < 0.5$ and $\beta < \alpha$, $p_c = 1 - \beta$. Fig.2 shows simulation results of our stochastic model, which are fully consistent with theoretical predictions [17].

To move from a model system [17] to a more realistic structure, we calculated the distribution of electron occupations for a chain, where hopping is allowed not only to/from the nearest V_o ($T = 0$, Fig. 3), and for systems, where hopping

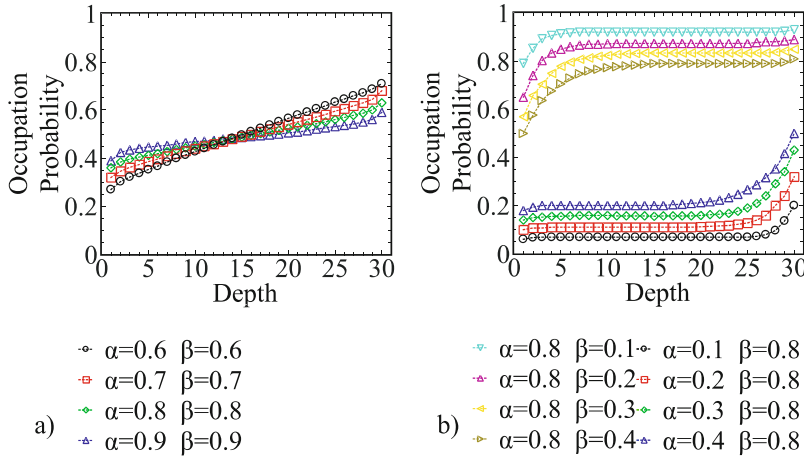


Fig. 3. Calculated distribution of electron occupation probabilities, if unidirectional hopping is allowed not only to/from the closest V_o ($T = 0$): (a) $\alpha > 0.5$ and $\beta > 0.5$; (b) $\beta < 0.5$ and $\beta < \alpha$; $\alpha < 0.5$ and $\alpha < \beta$

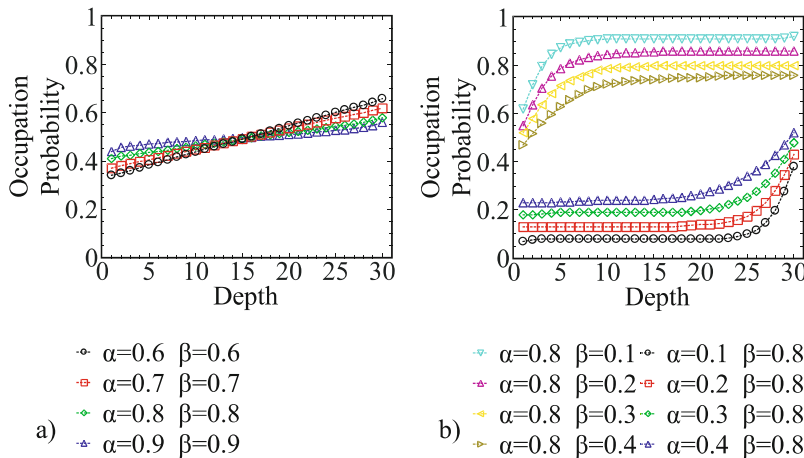


Fig. 4. Calculated distribution of electron occupation probabilities, for hopping according to (1-3), for $T > 0$: (a) $\alpha > 0.5$ and $\beta > 0.5$; (b) $\beta < 0.5$ and $\beta < \alpha$; $\alpha < 0.5$ and $\alpha < \beta$

(1-3) is allowed in both directions ($T > 0$, Fig. 4). Note that for $\alpha > 0.5$ and $\beta > 0.5$ (Fig. 3a and Fig. 4a) we still have $p_c = 0.5$ in the center, while for other values α, β we observe a decrease in p_c for $\alpha < \beta$ and an increase in p_c for $\beta < \alpha$.

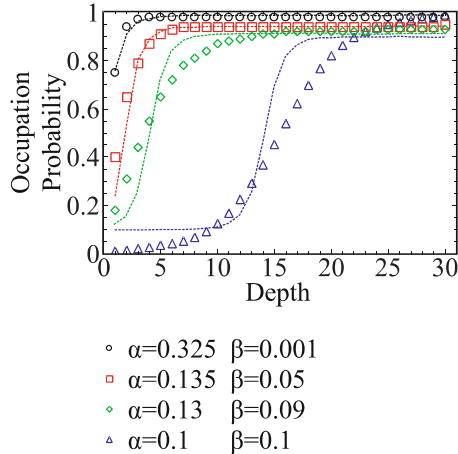


Fig. 5. Calculated distribution of electron occupation probabilities under different biasing voltages. Lines are from [12], symbols are obtained with our stochastic model.

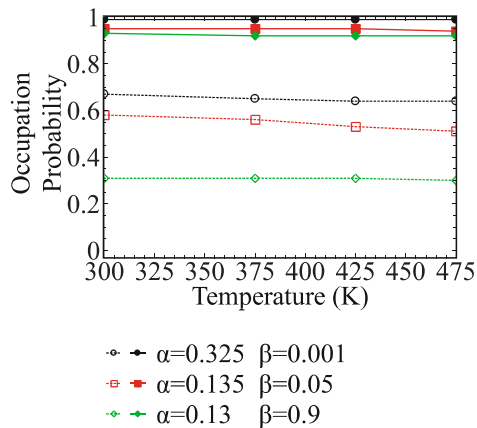


Fig. 6. Temperature dependence of electron occupation probability near the anode (line) and the cathode (dotted line)

We have calibrated our model in a manner to reproduce the results reported in [12], for $V = 0.6$ V to $V = 1.4$ V. Fig. 5 shows a case, when the hopping rate between two V_o is larger than the rate between the electrodes and V_o (i.e. $\alpha, \beta < 1$). In this case a low occupation region is formed near the cathode (bipolar behavior).

With the calibrated model we simulated the temperature dependence of the site occupations in the low occupation region. The results shown in Fig. 6 indicate high robustness of the low occupation region demonstrating changes of less than 10%, when the temperature is elevated from 25° C to 200° C.

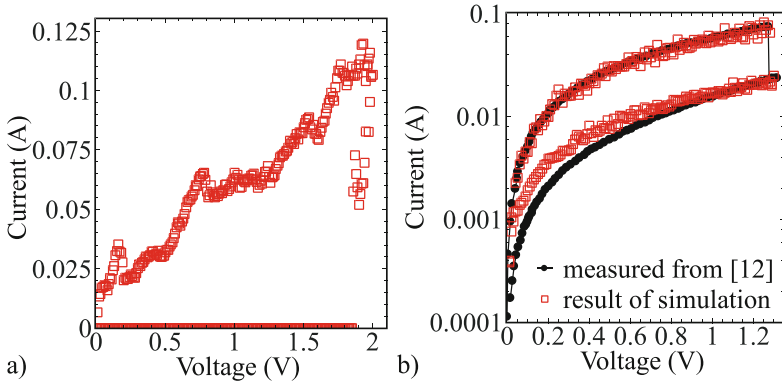


Fig. 7. $I - V$ characteristics for a single-CF device are obtained from our stochastic model: (a) SET $I - V$ characteristics; (b) RESET $I - V$ characteristics and measured results from [12]

3.2 Modeling of the SET and RESET Processes

For the simulations we have used a one-dimensional lattice consisting of thirty equivalent, equidistantly positioned hopping sites. To simplify calculations we assume that the coefficients of the boundary conditions are constant and equal to 0.1, independent of the applied voltage. In both simulations (SET and RESET process) we have used the same formation/annihilation energy for V_o . The result of the simulation of the SET process is shown in Fig. 7a.

To further demonstrate the capabilities of our model, we also simulated the RESET $I - V$ characteristics for a single-CF device [12]. For this purpose the CF was modified in such a way that for each V_o an oxygen ion is placed nearby. Fig. 7b. shows the simulation result of the stochastic model, which is in perfect agreement with measurements from [12].

4 Conclusion

In this work we have presented a stochastic model of the bipolar resistive switching mechanism. The distribution of the electron occupation probabilities calculated with the model is in excellent agreement with previous work. The simulated RESET process in RRAM is in good agreement with the experimental result. The proposed stochastic model can be used for performance optimization of RRAM devices.

Acknowledgments. This research is supported by the European Research Council through the grant #247056 MOSILSPIN.

References

1. Kryder, M.H., Kim, C.S.: After Hard Drives - What Comes Next? *IEEE Trans. on Mag.* 45(10), 3406–3413 (2009)
2. Kugeler, C., Nauenheim, C., Meier, M., et al.: Fast Resistance Switching of TiO₂ and MSQ Thin Films for Non-Volatile Memory Applications (RRAM). In: *NVM Tech. Symp.*, p. 6 (2008)
3. Chen, Y.S., Wu, T.Y., Tzeng, P.J.: Forming-free HfO₂ Bipolar RRAM Device with Improved Endurance and High Speed Operation. In: *Symp. on VLSI Tech.*, pp. 37–38 (2009)
4. Dong, R., Lee, D.S., Xiang, W.F., et al.: Reproducible Hysteresis and Resistive Switching in Metal-CuxO-Metal Heterostructures. *APL* 90(4), 42107/1-3 (2007)
5. Lin, C.C., Lin, C.Y., Lin, M.H.: Voltage-Polarity-Independent and High-Speed Resistive Switching Properties of V-Doped SrZrO₃ Thin Films. *IEEE Trans. on Electron Dev.* 54(12), 3146–3151 (2007)
6. Fujii, T., Kawasaki, M., Sawa, A., et al.: Hysteretic CurrentVoltage Characteristics and Resistance Switching at an Epitaxial Oxide Schottky Junction Sr-RuO₃/SrTi0.99Nb0.01O₃. *APL* 86(1), art. no. 012107 (2005)
7. Nian, Y.B., Strozier, J., Wu, N.J., et al.: Evidence for an Oxygen Diffusion Model for the Electric Pulse Induced Resistance Change Effect in Transition-Metal Oxides. *PRL* 98(14), 146403/1-4 (2007)
8. Wu, S.X., Xu, L.M., Xing, X.J.: Reverse-Bias-Induced Bipolar Resistance Switching in Pt/TiO₂/SrTi0.99Nb0.01O₃/Pt Devices. *APL* 93(4), 043502/1-3 (2008)
9. Szot, K., Speier, W., Bihlmayer, G., Waser, R.: Switching the Electrical Resistance of Individual Dislocations in Single-Crystalline SrTiO₃. *Nature Materials* 5, 312–320 (2006)
10. Nishi, Y., Jameson, J.R.: Recent Progress in Resistance Change Memory. In: *Dev. Res. Conf.*, pp. 271–274 (2008)
11. Xu, N., Gao, B., Liu, L.F., et al.: A Unified Physical Model of Switching Behavior in Oxide-Based RRAM. In: *Symp. on VLSI Tech.*, pp. 100–101 (2008)
12. Gao, B., Sun, B., Zhang, H., et al.: Unified Physical Model of Bipolar Oxide-Based Resistive Switching Memory. *IEEE Electron Dev. Let.* 30(12), 1326–1328 (2009)
13. Rozenberg, M.J., Inoue, I.H., Sanchez, M.J.: Nonvolatile Memory with Multilevel Switching: A Basic Model. *PRL* 92(17), 178302-1 (2004)
14. Kinoshita, K., Tamura, T., Aso, H., et al.: New Model Proposed for Switching Mechanism of ReRAM. In: *IEEE Non-Volatile Semicond. Memory Workshop 2006*, pp. 84–85 (2006)
15. Russo, U., Ielmini, D., Cagli, C., et al.: Conductive-Filament Switching Analysis and Self-Accelerated Thermal Dissolution Model for Reset in NiO-Based RRAM. In: *IEDM Tech. Dig.*, pp.775–778 (2007)
16. Sverdlov, V., Korotkov, A.N., Likharev, K.K.: Shot-Noise Suppression at Two-Dimensional Hopping. *PRB* 63, 081302 (2001)
17. Derrida, B.: An Exactly Soluble Non-Equilibrium System: The Asymmetric Simple Exclusion Process. *Phys. Rep.* 301(1-3), 65–83 (1998)